



## pH dependence of antibody: hapten association

Dennis Livesay<sup>a,b</sup>, Scott Linthicum<sup>d</sup>, Shankar Subramaniam<sup>b,c,\*</sup>,<sup>1</sup>

<sup>a</sup>Department of Chemistry, University of Illinois at Urbana-Champaign, Urbana, IL 61801, USA

<sup>b</sup>National Center for Supercomputing Applications, University of Illinois at Urbana-Champaign, Urbana, IL 61801, USA

<sup>c</sup>Departments of Biochemistry, Chemical Engineering, and Molecular and Integrative Physiology, Center for Biophysics and Computational Biology, and Beckman Institute for Advanced Science and Technology, University of Illinois at Urbana-Champaign, Urbana, IL 61801, USA

<sup>d</sup>Department of Veterinary Pathobiology, College of Veterinary Medicine, College of Science, Texas A&M University, College Station, Texas, TX 77843, USA

Received 16 November 1998; accepted 1 February 1999

### Abstract

Monoclonal antibody NC6.8 is specific for the superpotent sweetener, N-(*p*-cyanophenyl)-N'-(diphenylmethyl)-guanidiniumacetic acid. The three-dimensional structure of the complex shows the close proximity of complementary charged residues on the antibody and groups of the hapten. As a result, association is dependent on the pH, dielectric, and ionic strength of the medium. Continuum electrostatics methods are used to calculate the pH-dependent association energetics of NC6.8 with the superpotent sweetener. In addition to providing a titration profile, the calculations quantitatively assess the relative influence of charged groups on the energetics of association. Models of site directed mutants are constructed to probe the influence of each charged interface residue on the pH-dependent energetics of association. Examination of electrostatic contribution to free energy of association in mutant complexes, where the key acidic residues on the antibody are neutralized, shows that charge complementarity at the combining site is an important requirement for hapten binding. Also, based on the pK<sub>a</sub> values of several combining site tyrosine residues, aromatic  $\pi$ -stacking and van der Waal's contacts between the antibody and hapten contribute to the specificity of the complex. © 1999 Elsevier Science Ltd. All rights reserved.

**Keywords:** Electrostatics; Poisson–Boltzmann equation; pK<sub>a</sub>; Titration curves; Molecular recognition; Salt bridges; Antibody; Hapten

### 1. Introduction

Molecular association between a biological receptor and ligand is highly specific. The overall reaction is a delicate balance between attractive and repulsive forces. Complex formation occurs at the cost of removing waters from the binding site and reducing sidechain degrees of freedom, which is balanced by the energy gain due to non-covalent interactions, burying of hydrophobic surfaces, and other stabilizing factors. At long distances, electrostatic forces orient and steer

the ligand to the receptor, providing the leit-motif for association (Kozack et al., 1995). The amount of stabilization incurred on association is determined by many factors, each influencing the total interaction energy (Morokuma, 1977). Much work has been done in the area of thermodynamic component analysis (Boresch et al., 1994; Boresch and Karplus, 1995; Brady et al., 1996), where the free energy is broken down into terms of specific interactions. The components generally implicated are electrostatic interactions, van der Waals interactions, and hydrophobic contacts. Using continuum electrostatic models, some of these components can be modeled.

Three-dimensional structures for a variety of antibody Fab fragments and antibody-antigen complexes have been solved (for a review see Padlan, 1994). Antigen recognition is generally mediated by 15–20

\* Corresponding author.

<sup>1</sup>Address reprint requests to Shankar Subramaniam, Beckman Institute, University of Illinois at Urbana-Champaign, 405 N. Mathews Avenue, Urbana, Illinois 61801, shankar@ncsa.uiuc.edu

amino acids (Poljak et al., 1973; Davies and Metzger, 1983; Padlan, 1990), most of which are from six peptide loops that make up the complementary determining region (CDR). The CDR binding site is formed by the anti-parallel  $\beta$ -strand turns of the variable regions of the heavy and light chains (Chothia and Lesk, 1987). Mutagenesis of single residues at the combining site of the antibody or antigen often results in a large loss of specificity (Knossow et al., 1984; Alegre et al., 1992; Chacko et al., 1995). Association between antibody and antigen is often mediated by charged residues, resulting in the energetics being strongly pH-dependent. In a previous study (Gibas et al., 1997) we have used continuum electrostatic calculations to calculate the pH dependence of antibody:antigen association. Two antibody:lysozyme complexes were studied (D44.1 and HyHEL-5). In both complexes, association is stabilized by conserved charge-mediated interactions at the combining site. The local environment surrounding the combining has significant effects on the association energetics. The factors affecting the energetics include minor structural rearrangements, buried interfacial area, dielectric environment of key charged residues, and geometry of the interacting residues. Comparisons of calculated pH dependent behavior showed good agreement with experimental results (Tello et al., 1993; Benjamin et al., 1992).

Anchin and Linthicum (1993) have produced a library of monoclonal antibodies against the superpotent guanidino sweet tasting ligand, N-(*p*-cyanophenyl)-N'-(diphenylmethyl)-guanidiniumacetic acid. Using intrinsic fluorescence spectroscopy Droupadi et al. (1992) found the affinity of one of these mAb to be in the nanomolar range, which is nearly equal to the putative receptor affinity for the sweet taste ligand. Circular dichroism and absorption spectroscopy results suggest participation of aromatic residues in complex formation (Tetin and Linthicum, 1996; Droupadi and Linthicum, 1995). Gudatt et al. (1994) have solved the X-ray structure of NC6.8 fab fragment in the complexed (2.2 Å) and uncomplexed (2.7 Å) forms. The results from the X-ray studies support the results of the earlier work.

In this paper we report the results from continuum electrostatic calculations of the pH-dependent energetics of mAb NC6.8:N-(*p*-cyanophenyl)-N'-(diphenylmethyl)-guanidiniumacetic acid association. Individual pKa values of antibody residues and charged groups on the hapten in the bound and free state are reported. Residues that show significant changes in pKa values on complex formation are examined in order to understand the chemical basis of the recognition phenomena. Also, we attempt to delineate those changes in pKa values due to the electrostatics of hapten recognition as opposed to those due to the structural rearrangement of the antibody upon complex formation.

## 2. Materials and methods

### 2.1. Calculation of protein pKa values

The method of Tanford and Roxby (Tanford and Roxby, 1972) assumes that equilibrium between acid and base is governed by the intrinsic pKa of each site, where  $\text{pK}_{\text{int},i}$  is equal to the pKa at site  $i$  if every site in the protein were neutral. The actual pKa is equal to the intrinsic pKa minus a term that represents the deviation from the intrinsic state. This deviation is governed by the pairwise electrostatic interaction between the residue in question and every other residue. The pKa value of each site is evaluated by

$$\text{pKa}_i = \text{pK}_{\text{int},i} - (2.303k_B T)^{-1} \sum_{k=1}^n \Delta G_{ik}(q_k^0 + \theta_k) \quad (1)$$

where  $\Delta G_{ik}$  is equal to the interaction free energy between  $i$  and  $k$ ,  $q_k$  is the fractional ionization of site  $k$ . For  $n$  titratable sites, this method requires the computationally expensive enumeration of  $2^n$  states. In order to make the pKa calculation feasible, several modified Tanford and Roxby schemes have been developed.

The method of Gilson (1993) and Antosiewicz et al. (1994) uses clustering of titrating sites to reduce the computational expense of the pKa calculation. The cluster method exactly solves the ionization polynomial within a cluster, and uses a mean field approximation to treat intercluster interactions. This method is part of the University of Houston Brownian Dynamics (UHBD) suite of programs (Madura et al., 1995).

In the pKa calculation, a pairwise electrostatic potential exists between site  $i$ , and every other group  $j$ , according to its average charge,  $\langle q_j \rangle$ . Both, the cluster method and the more general method of Tanford and Roxby express the ionization free energy as the free energy difference between a hypothetical neutral state and some ionization state  $\alpha$ . The ionization free energy is calculated from (2) (Schellman, 1975),

$$G_{\text{ion}} = -RT \ln \Sigma \quad (2)$$

where  $\Sigma$  is the ionization polynomial. In the mean field approximation (cluster method), the ionization polynomial for a single cluster is given by the expression

$$\Sigma_I = \sum_{\alpha=0}^{2^{n_I}-1} \left( e^{-\beta \sum_{i=1}^{n_I} G_{\text{elec},\alpha}^i} e^{-\beta \sum_{k \in I} \theta_k G_{ik}} \right) \times \prod_{i=1}^{n_I} K_{\text{ai}}^{-x_{\alpha} z(i)} [H^+]^{z(i)} \quad (3)$$

where the outer sum is over the ionization states of the cluster  $I$  only, and  $k$  is summed over all other clusters.

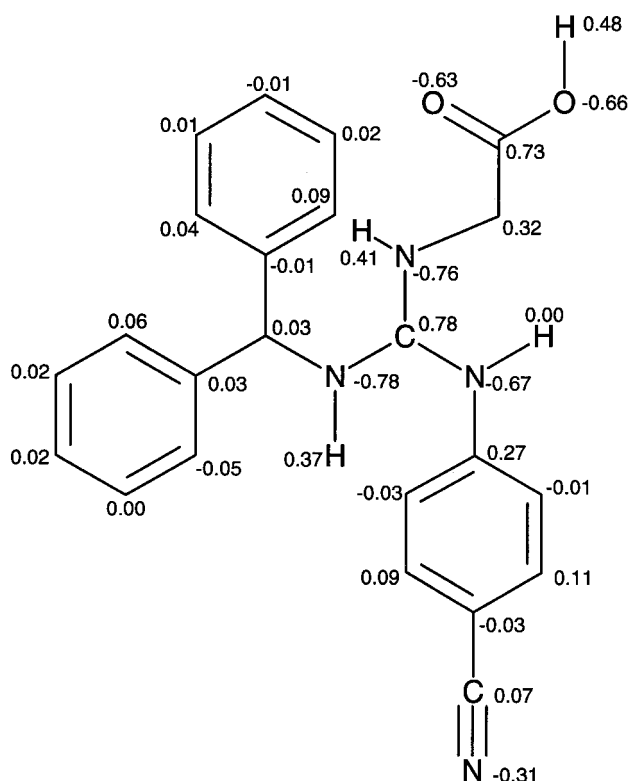


Fig. 1. Calculate partial charges of the sweetener, N-(*P*-cyanophenyl)-*N'*-(diphenylmethyl)-guanidiniumacetic acid, using the Gaussian96 package with the 6-31G basis set.

$G_{\text{elec},\alpha}$  is the purely electrostatic contribution to the free energy,  $K_{ai}$  is the acid equilibrium constant for each titrating site, and  $\theta_k \Delta G_{ik}$  is influence of  $k$  on  $i$  in the mean field approximation ( $\theta_k$  is the fractional ionization at  $k$ ). Each site is described by a pair of vectors,  $x_\alpha(i)$  and  $z(i)$ , such that  $x_\alpha(i)$  is equal to  $-1$  for an acid and  $+1$  for a base and  $z(i)$  is equal to zero for the neutral state and  $+1$  for the ionized. The electrostatic free energy is given by the expression

$$G_{\text{elec},\alpha} = \sum_{i=1}^m x_\alpha(i) \left[ \Delta \Delta G_i + \sum_{j>i}^m x_\alpha(j) \Delta G_{ij} \right] \quad (4)$$

The  $\Delta \Delta G_i$  term is the extra free energy relative to the unperturbed state of titrating group  $i$  when all other titrating sites are neutral, and  $\Delta G_{ij}$  is equal to the extra free energy of ionizing site  $i$  due to the presence of titrating sites  $j$ .

For all calculations, the partial-charges used in the calculation of the electrostatic energies were taken from the CHARMM parameter set (Brooks et al., 1983) and radii from the Optimized Parameters for

Liquid Systems (Jorgensen and Tirado-Rives, 1988). The partial charges of the ligand were calculated using Gaussian96 package with the 6-31G basis set (Fig. 1). The model pKa values for titratable amino acids are taken from Antosiewicz et al. (1994) and are set at 4.0 and 12.4 for the carboxy and guanidinium moieties of the hapten, respectively. The temperature, ionic strength, and ionic radius remained constant for all calculations at 298 K, 150 mM, and 2.0 Å, respectively. The choice of interior protein dielectric has been debated in the recent literature. We have found that an interior dielectric of 20 gives the best results (Gibas and Subramaniam, 1996; Antosiewicz et al., 1994). All calculations reported here use a protein interior dielectric of 20 and solvent dielectric of 80. The finite grid spacing begins at 1.5 Å, and is then focused to 1.2, 0.75, and 0.25 Å. The boundary between solvent and protein dielectrics is differentiated using the method of Shrake and Rupley (Shrake and Rupley, 1957), with a probe radius of 1.4 Å.

## 2.2. Protein structures

The protein structures used in the pKa calculations are modified versions of the coordinates received from Guddat et al. (1994). The results from three structures are presented here. Those structures are NC6.8 without ligand (2.7 Å), NC6.8 with ligand (2.2 Å), and the complexed NC6.8 structure with the ligand coordinates removed from the structure file (see below). The structures are modified in the same manner as previously published works from this laboratory (Gibas and Subramaniam, 1996) to only include the Fv fragment, hapten, and 100% solvent inaccessible water (henceforth referred to as structural water). In order to negate changes in pKa values due to structural rearrangement of the antibody on association, uncomplexed structures were created from the complexed structures. From the Fv fragments of complexed NC6.8, the coordinates pertaining to the hapten were deleted, resulting in an antibody structure exactly the same as the complexed antibody structure. Henceforth, structures created in this manner will be designated pseudo-apoprotein structures, whereas uncomplexed structures from experiment will be simply designated as apoprotein structures. The continuum method implemented in UHBD uses explicit polar hydrogen atoms in the pKa calculation. Polar hydrogens were added using the program HBUILD within Quanta96.<sup>2</sup>

Several mutant structures are also studied. The mutants studied are designed to minimize differences in the sidechain structures so as to avoid large perturbations from the experimentally determined native structures. Seven types of mutations are presented here, Glu → Gln, Gln → Glu, Asp → Asn, Asn → Asp,

<sup>2</sup> Quanta96 is a molecular modeling and display program developed by Molecular Simulations, Inc., 200 Fifth Ave., Waltham, MA 02254.

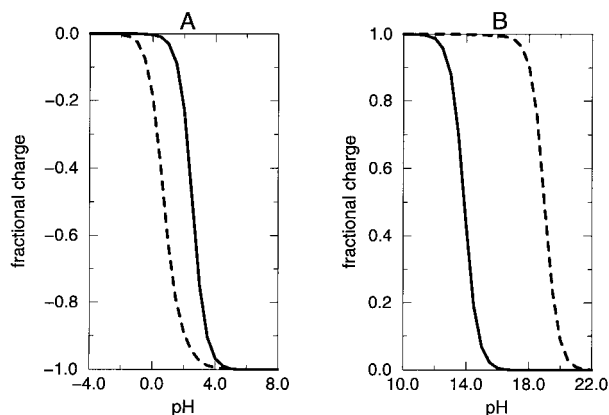


Fig. 2. Titration curves of free (solid) and bound (dashed) *N*-(*p*-cyanophenyl)-*N'*-(diphenylmethyl)-guanidiniumacetic acid. (A) Acetic acid moiety. (B) Guanidinium moiety.

Tyr → Phe, Arg → Ala, and Glu → Asp. All are structurally conserved mutations, and were constructed (except for the Glu → Asp mutations) by editing the PDB file and then using HBUILD to place the polar hydrogen atoms back in the correct locations. No minimization was run on the mutated structures. The

Glu → Asp mutated structures were built using the mutate protein option in Quanta96. Control mutations of each type are also presented to ensure the reliability of the above techniques.

### 3. Results

#### 3.1. Hapten structure and titrating behavior

The *N,N,N'*-trisubstituted sweetener is selected as a model of sweetener–receptor interactions due to its remarkable potency. The sweet taste molecule is more than 200,000 times sweeter than sucrose as revealed by a threshold taste test (Muller et al., 1992). It has been shown that the *p*-cyanophenyl ring is necessary for such high affinity, and has been hypothesized that its high affinity can be explained by  $\pi$ -stacking with aromatic residues of the receptor. The sweetener has two titrating sites, the carboxylate and the guanidinium moieties. In solution the sweetener exists as a zwitterion. Fig. 2 shows the calculated titration behavior of the unbound hapten. We have not been able to find any titration studies of the sweetener in the literature,

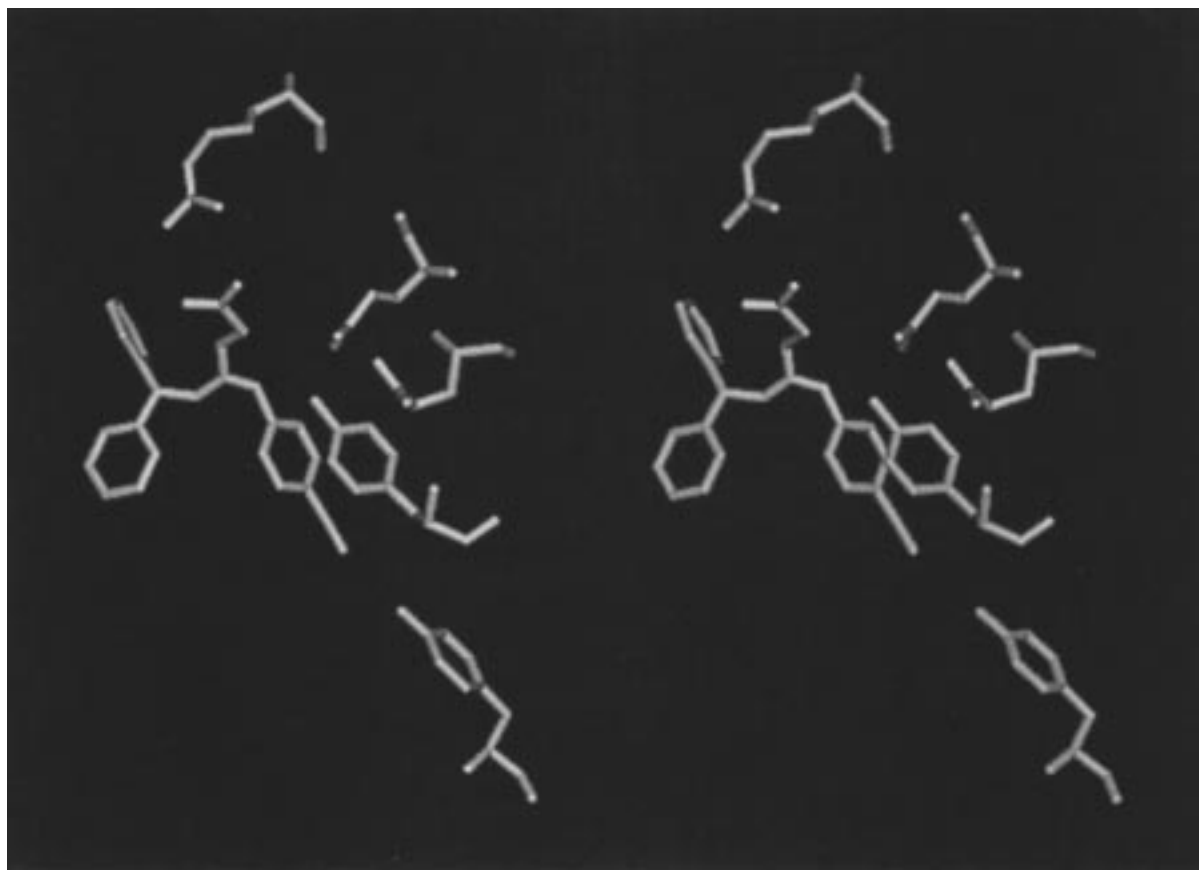


Fig. 3. Side-by-side stereo view of key combining site residues and ligand of the native NC6.8, *N*-(*p*-cyanophenyl)-*N'*-(diphenylmethyl)-guanidiniumacetic acid complex.

Table 1  
Intra-antibody distances<sup>a</sup>

| Residue      | Carboxylate carbon | Guanidinium carbon | <i>p</i> -Cyanophenyl nitrogen |
|--------------|--------------------|--------------------|--------------------------------|
| His L:31 NDI | 8.02               | 7.03               | 9.84                           |
| Tyr L:37 OH  | 10.03              | 8.10               | 12.92                          |
| Tyr L:41 OH  | 14.80              | 11.67              | 4.21                           |
| Tyr L:101 OH | 4.94               | 4.14               | 6.85                           |
| Glu H:35 CD  | 8.65               | 6.78               | 6.27                           |
| Glu H:50 CD  | 5.04               | 4.86               | 8.47                           |
| Arg H:57 CZ  | 4.05               | 7.20               | 14.71                          |
| Tyr H:100 OH | 11.59              | 9.08               | 9.87                           |
| Asp H:104 CG | 15.46              | 12.06              | 9.06                           |

<sup>a</sup> Distances (Å) between combining site residues and ligand in the NC6.8, N-(*p*-cyanophenyl)-N'-(diphenylmethyl)-guanidiniumacetic acid complex.

but it should be very near the unsubstituted parent compound, guanidiniumacetic acid, in which the acetic acid moiety pKa is 2.82 (Langes Handbook of Chemistry, 14th ed. 1992), similar to our calculated value of 2.53. On complex formation, both sites get shifted far away from neutral; in fact, the calculated pKa value of the carboxylate moiety in the complexed structure is 0.73, whereas the pKa value of the guanidinium moiety is 19.0.

### 3.2. NC6.8, hapten structures

Fig. 3 shows the stereo image of the key residues at the antibody combining site. Table 1 summarizes the distances between nine key combining site residues and the bound ligand. The carboxyl moiety of the sweetener is involved in a salt link with the sidechain guanidinium ion of Arg H:57. The amide sidechain of Asn H:59 is also hydrogen bonded to one of the carboxylic oxygens of the sweetener with a separation of 2.83 Å. The guanidinium ion moiety of the sweetener is electrostatically interacting with the side chain carboxyl of Glu H:50 (3.28 Å) and is hydrogen bonded to the backbone carbonyl of Tyr H:100 (2.91 Å). The *p*-cyanophenyl moiety is electrostatically bonded to Tyr L:41 and Ser L:94 through a series of 100% buried bridging water molecules.

$\pi$ -stacking interactions also play a large role in the specificity of the association. The sweetener is made up of three phenyl rings, and there are no less than 14 aromatic residues within a 15 Å sphere about the hapten. HBPLUS (McDonald and Thornton, 1994) specifically implicates four aromatic residues as being involved in hydrophobic contact with the hapten. Tyr L:101 is involved in extensive  $\pi$ -stacking interactions with the *p*-cyanophenyl moiety of the sweetener, Tyr L:37 is in contact with one phenyl of the diphenylmethyl moiety, whereas Tyr H:100 is contacting the other. Trp H:33 is involved in a van der Waal's con-

tact with both carbons of the acetic acid moiety of the sweetener.

There are also a large number of charged residues within the 15 Å sphere about the hapten. There are seven basic and four acidic residues at the binding site. However, three of the basic residues are histidines which are neutral at physiological pH. Therefore, at pH 7.0, there is charge compensation between the antibody and hapten.

### 3.3. Changes on complex formation

Fig. 4 shows the superimposed structures of the unbound antibody and the NC6.8:N-(*p*-cyanophenyl)-N'-(diphenylmethyl)-guanidiniumacetic acid complex. There are significant structural differences between the



Fig. 4. Superimposed structures of the apoprotein NC6.8 and the NC6.8, N-(*p*-cyanophenyl)-N'-(diphenylmethyl)-guanidiniumacetic acid complex.

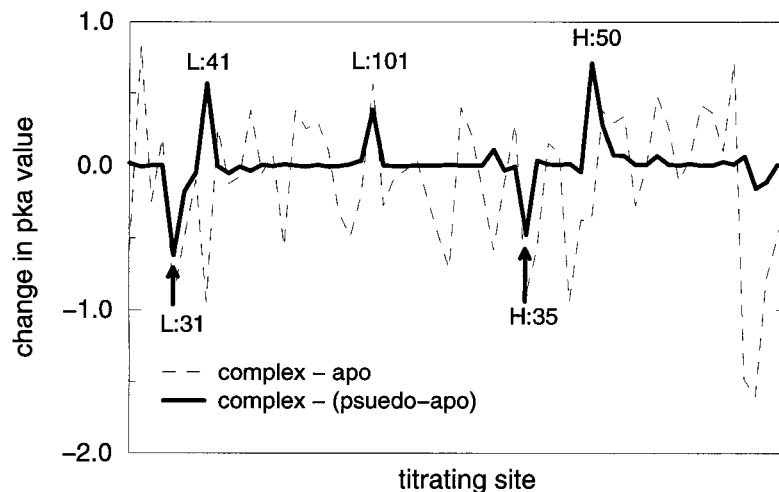


Fig. 5. Calculated pKa shifts on complex formation for the wild-type and pseudo-apoprotein structures vs residue number.

two structures (RMS=0.69 Å for  $\alpha$ -carbons and 1.42 Å for all atoms). Large amounts of changes in pKa values at nearly every titratable residue arise from structural and electrostatic differences between the complexed and free antibodies. Delineating which changes, are a result of structural changes and which changes are due to association is our first goal. By comparing the complexed structure with the pseudo-apoprotein, the sites electrostatically affected by association can easily be determined. The changes in pKa between the complex structure and the pseudo-apoprotein structure (Fig. 5) are only a result of complex formation. The changes are localized to titrating residues at the combining site, whereas those further away are unchanged.

### 3.4. Wild-type NC6.8, hapten complex

Table 2 summarizes the calculated changes in pKa values on complex formation. All titrating sites that have significant shifts in pKa values (more than  $\pm 0.125$

Table 2  
Effects of association of pKa values<sup>a</sup>

| Residue   | $\Delta$ pKa |
|-----------|--------------|
| His L:31  | -0.619       |
| Tyr L:37  | -0.176       |
| Tyr L:41  | 0.569        |
| Tyr L:101 | 0.387        |
| Glu H:35  | -0.479       |
| Glu H:50  | 0.710        |
| Arg H:57  | 0.280        |
| Tyr H:100 | -0.158       |
| Asp H:104 | -0.112       |

<sup>a</sup> Significant changes in pKa values of the wild-type NC6.8, N-(*p*-cyanophenyl)-N'-(diphenylmethyl)-guanidiniumacetic acid complex on association (complex-free).

pH units) are within a 15 Å sphere centered at the guanidinium carbon of the hapten. Glu H:50 has the largest shift on complex formation, supporting earlier

Table 3  
The effects of association of solvent accessibility<sup>a</sup>

| Residue   | $\Delta$ Solvent accessibility |  |
|-----------|--------------------------------|--|
|           | Whole residue (%)              | Titrating atom (Å <sup>2</sup> )         |
| His L:31  | -10.1                          | 0.00 (NDI)<br>-10.98 (NE2)               |
| Asn L:33  | -6.7                           | -  |
| Tyr L:37  | -4.7                           | -5.15                                    |
| His L:39  | -1.5                           | 0.00 (NDI)<br>0.00 (NE2)                 |
| Tyr L:41  | -0.6                           | -1.17                                    |
| Ser L:94  | -2.2                           | -  |
| Gln L:95  | -0.2                           | -  |
| Gly L:96  | -23.3                          | -  |
| Val L:99  | -1.1                           | -  |
| Tyr L:101 | -14.8                          | -13.11                                   |
| Glu H:31  | -1.4                           | 0.00 (OE1)<br>0.00 (OE2)                 |
| Trp H:33  | -15.0                          | -  |
| Glu H:35  | -3.1                           | -0.01 (OE1)<br>-0.31 (OE2)               |
| Glu H:50  | -4.6                           | -1.06 (OE1)<br>-5.90 (OE2)               |
| Leu H:52  | -4.4                           | -  |
| Arg H:57  | -10.9                          | 0.00 (NE)<br>-5.02 (NH1)<br>-20.99 (NH2) |
| Asn H:59  | -7.7                           | -  |
| Gly H:99  | -4.1                           | -  |
| Tyr H:100 | -31.6                          | -5.60                                    |
| Ser H:101 | -15.7                          | -  |
| Ser H:102 | -4.6                           | -  |
| Met H:103 | -5.6                           | -  |

<sup>a</sup> Differences in residue solvent accessibility of the wild-type NC6.8, N-(*p*-cyanophenyl)-N'-(diphenylmethyl)-guanidiniumacetic acid complex on association (complex-free).

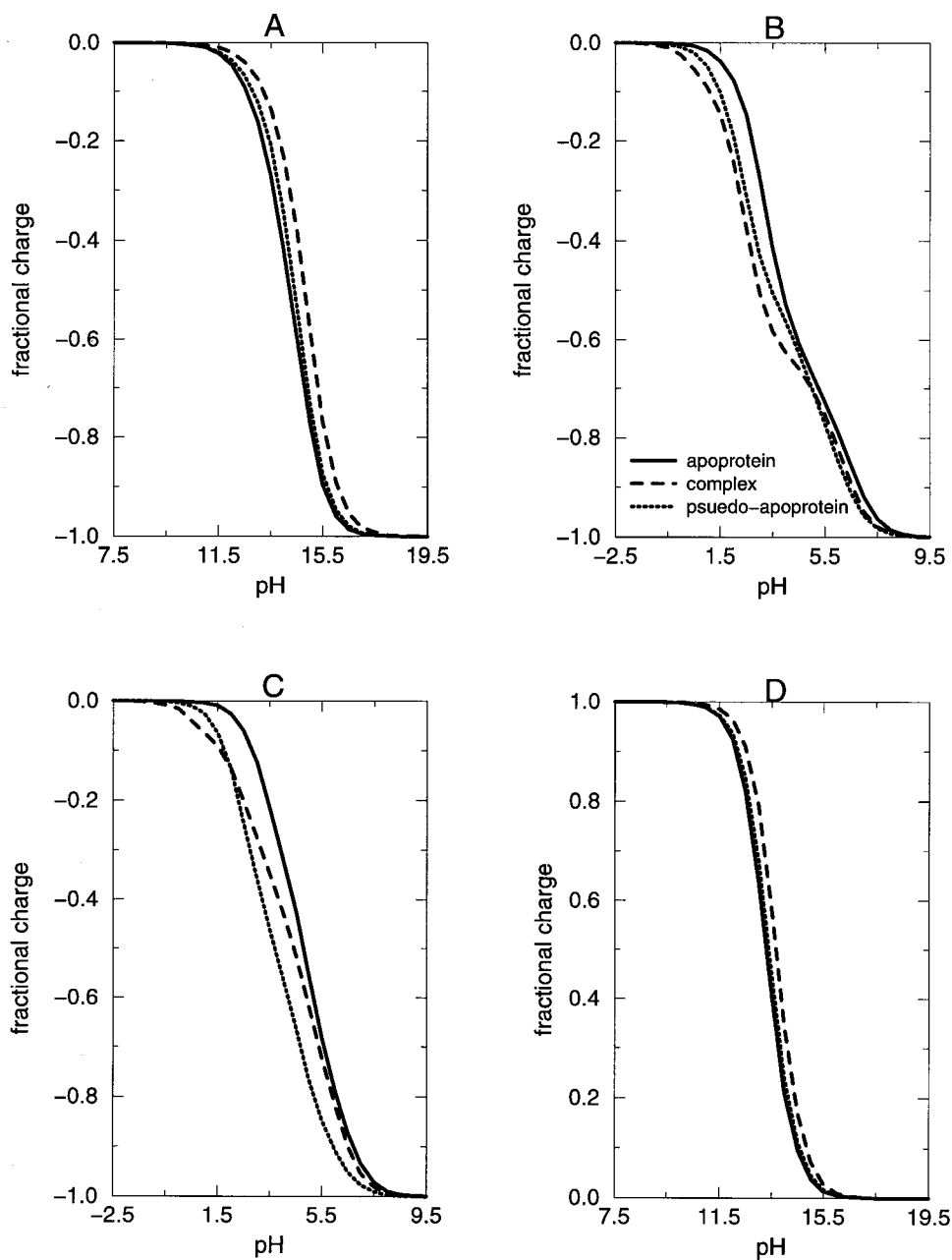


Fig. 6. Titration curves of key residues in the native apoprotein, pseudo-apoprotein, and complexed structures. (A) Tyr L:101. (B) Glu H:35. (C) Glu H:50. (D) Arg H:57.

predictions of its importance to ligand affinity. Another glutamate residue (H:35) also has a large change in pKa value on complex formation, suggesting that it could also be interacting with the ligand. In all, nine residues have significant changes in pKa values. Of these, all changes can be explained by either electrostatic interactions with the ligand or by decreased solvent accessibility on complex formation (Table 3). Fig. 6 shows the titration curves of the ligand and the four most important residues that define ligand specificity, Tyr L:101, Glu H:35, Glu H:50, and ARG H:57.

The pairwise electrostatic potentials between key titrating sites are summarized in Fig. 7. These are the site-site interaction energies,  $\Delta G_{ij}$  [Eq. (4)], obtained from the pKa calculation. The interaction energy (kcal/mol) is the quantitative measure of how much one site effects the pKa value of another. The summation of all non-zero interaction energies (plus the self-ionization term) results in the total pKa shift for a particular. The typical interaction energy is less than 0.4 kcal/mol, however for particularly strong interactions, the value can equal as much as 1.5 kcal/mol. all sites with significant changes in pKa values on com-

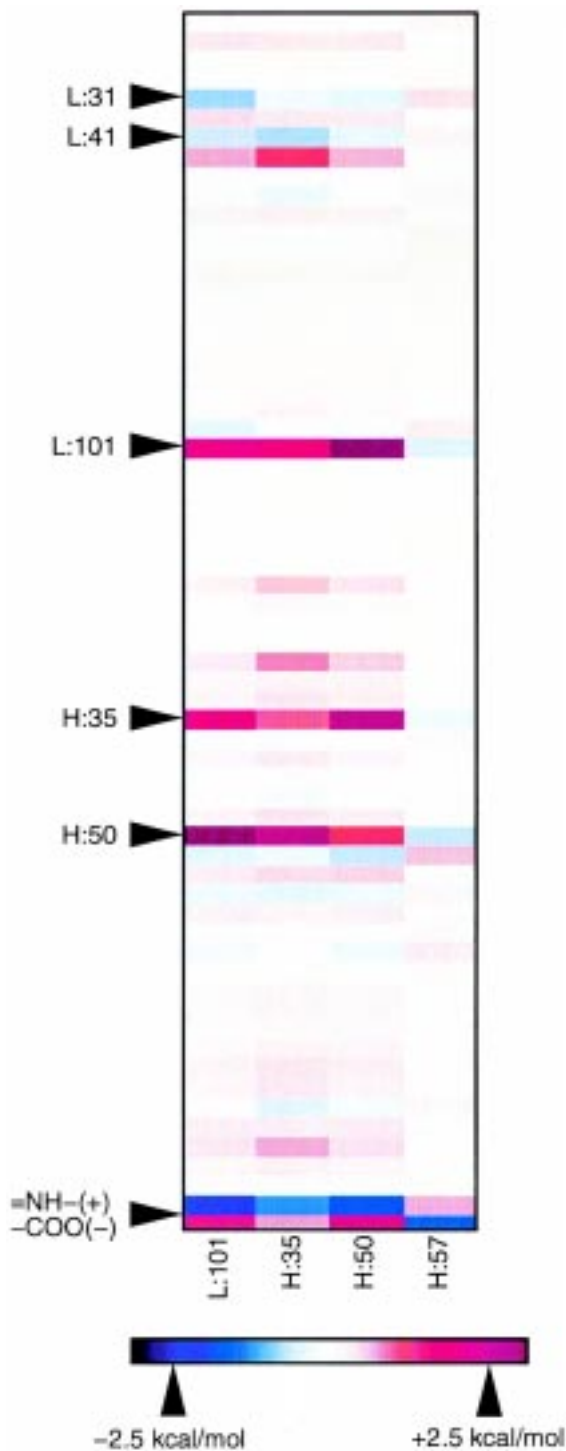


Fig. 7. Electrostatic interaction matrix of the NC6.8, N-(*p*-cyanophenyl)-N'-(diphenylmethyl)-guanidiniumacetic acid complex. The value plotted is the interaction energy,  $W_{ij}$  [Eq. (3)], for each pair of titrating sites, in kcal/mol. Favorable interactions are presented in blue, whereas unfavorable interactions are given in red. All titrating sites (with key sites labeled) are plotted against the four key combining site residues.

plex formation have large site–site interaction energies between themselves and the hapten.

Table 4  
pKa value changes of mutant structures<sup>a</sup>

| Mutation           | Residue    | Change |
|--------------------|------------|--------|
| Y(L:37)F           | Tyr L:41   | 1.073  |
|                    | Lys L:50   | 0.490  |
|                    | Arg L:55   | 0.652  |
|                    | Tyr L:101  | 0.538  |
|                    | Tyr H:27   | 0.416  |
|                    | Tyr H:94   | 0.511  |
|                    | Tyr H:95   | 0.498  |
| Y(L:41)F           | guanidinio | 0.434  |
|                    | Tyr L:101  | 0.470  |
| Y(L:101)F          | Glu H:35   | -0.496 |
|                    | Glu H:50   | 0.971  |
| E(H:35)Q           | guanidinio | 1.315  |
|                    | Tyr L:41   | 1.204  |
|                    | Tyr L:101  | 1.186  |
|                    | Tyr H:27   | 0.561  |
|                    | Glu H:50   | 1.470  |
| E(H:35)D           | guanidinio | 0.748  |
|                    | Glu H:50   | 0.715  |
| E(H:50)Q           | Tyr L:101  | 2.394  |
|                    | Glu H:35   | 0.625  |
| E(H:50)D           | guanidinio | 1.084  |
|                    | Tyr L:101  | 1.307  |
| E(H:35)Q, E(H:50)Q | Glu H:35   | -1.100 |
|                    | His L:39   | 0.675  |
| E(H:35)D, E(H:50)D | Tyr L:41   | 1.589  |
|                    | Tyr L:101  | 3.627  |
|                    | Tyr H:27   | 0.845  |
|                    | guanidinio | 1.810  |
|                    | Tyr L:101  | 1.634  |
| R(H:57)K           | Glu H:50   | -0.562 |
|                    | guanidinio | -1.302 |
| N(H:59)D           | Tyr L:101  | -1.110 |
|                    | Glu H:50   | -2.342 |
|                    | carboxyl   | -0.530 |

<sup>a</sup> Significant changes in pKa values ( $pK_{a_{wt}} - pK_{a_{mutant}}$ ) of selected mutant NC6.8, N-(*p*-cyanophenyl)-N'-(diphenylmethyl)-guanidiniumacetic acid complexes. The guanidinium moiety of the hapten is labeled guanidinio and the acid moiety of the hapten is labeled carboxyl.

We have previously reported (Gibas and Subramaniam, 1996) that inclusion of solvent inaccessible (or nearly inaccessible) water molecules may improve results of the pKa calculation in some cases. In this calculation water molecules calculated to be 100% buried by Naccess (Hubbard et al., 1991) were included. Only the  $\Delta pK_a$  values of Glu H:35 and Glu H:50 are modified slightly (0.199 and -0.156 pH units, respectively) by including structural waters in the calculation.

### 3.5. Selected mutants

Significant changes in pKa values due to selected mutations are listed in Table 4. The largest of the shifts is nearly four pH units, although the typical change is around a single pH unit. In all cases, the changes in pKa values can be directly attributed to

Table 5  
The effects of mutations on pairwise potentials<sup>a</sup>

|                      | E(H:35)D | E(H:50)D | E(H:35)D; E(H:50)D |
|----------------------|----------|----------|--------------------|
| H:35-L:101           | 0.25     | −0.05    | 0.20               |
| H:35-H:50            | 0.53     | 0.28     | 0.64               |
| H:50-L:101           | 0.04     | 0.77     | 0.80               |
| H:35-Lig guanidinium | −0.14    | 0.00     | −0.12              |
| H:35-Lig carboxy     | 0.10     | 0.00     | 0.06               |
| H:50-Lig guanidinium | 0.00     | −0.38    | −0.40              |
| H:50-Lig carboxy     | 0.00     | 0.22     | 0.23               |

<sup>a</sup> Differences in the pairwise potentials ( $\Delta\theta_{wt-mutant}$  kcal/mol) of key combining site residues.

local changes in the electrostatic interactions of the mutation studied. The typical change of pKa values of sites far away from the mutated residue is much below a quarter pH unit.

Mutation of Glu H:35 to a glutamine residue results in pKa shifts of several key residues, including Glu H:50 and Tyr L:101. Mutating Glu H:50 to glutamine causes a large pKa shift in Tyr L:101. The double mutation of both glutamate residues to glutamines has the most affect on pKa value changes. Shortening of the Glu H:50 by a methylene group (i.e., mutating to Asp) causes a large pKa shift in Tyr L:101, but the mutation has no significant effects on any other residues other than Glu H:50.

Table 5 describes how mutating the two key glutamates to aspartate residues affects the local pairwise potentials. Shortening Glu H:35 by a methylene group (E(H:35)D) causes the electrostatic pairwise potential between the acidic residue at H:35 and the guanidinium to be raised by 0.14 kcal/mol. Whereas, the pairwise potential between H:35 and the ligand's carboxyl group is stabilized by 0.1 kcal/mol, resulting in an overall destabilized pairwise potential between Asp H:35, ligand compared to Glu H:35, ligand. Shortening Glu H:50 by a methylene group (E(H:50)D) has the same type of effects as the H:35 mutation, however the sum of the two H:50, ligand pairwise potentials are more repulsive in the E(H:50)D mutation.

### 3.6. pH-dependent association energetics

Fig. 8 shows the electrostatic potentials of the native, uncomplexed NC6.8 structure mapped onto the molecular surface. The anionic well at the center of Fig. 8A is from the negatively charged Glu H:35 and Glu H:50. The cationic extension flagging the anionic well is from the positively charged Arg H:57. Large visible differences arise from the series of glu → gln mutations in Fig. 8B–D, disrupting the charge complementarity of the Ab, hapten complex. The results of the pKa calculations allows us to quantify the visual differences.

Table 6  
Effects of mutations on the electrostatic free energy of association<sup>a</sup>

|                        | $\Delta(\Delta G_{elec,cmplx-free antibody})_{wt-mutant}$ kcal/mol |
|------------------------|--|
| D(L:17)N <sup>b</sup>  | −0.31  |
| D(H:104)N              | −0.80  |
| E(L:110)Q <sup>b</sup> | −0.08  |
| E(H:35)Q               | 0.09   |
| E(H:35)D               | −0.33  |
| E(H:50)Q               | −0.19  |
| E(H:50)D               | 0.29   |
| E(H:35)Q; E(H:50)Q     | −1.05  |
| E(H:35)D; E(H:50)D     | 0.06   |
| N(L:35)D               | −0.23  |
| N(H:59)D               | −0.38  |
| N(H:77)D <sup>b</sup>  | −0.29  |
| Q(L:95)E               | −0.41  |
| Q(H:118)E <sup>b</sup> | 0.14   |
| R(H:40)A <sup>b</sup>  | 0.16   |
| R(H:57)A               | −0.45  |
| Y(L:37)F               | 0.00   |
| Y(L:41)F               | 0.10   |
| Y(L:91)F <sup>b</sup>  | 0.08   |
| Y(L:101)F              | 0.15   |
| Y(H:100)F              | 0.14   |

<sup>a</sup> Differences in the change of free energy on NC6.8, N-(*p*-cyanophenyl)-N'-(diphenylmethyl)-guanidiniumacetic acid complex formation due to various mutations (neutral pH).

<sup>b</sup> Indicates control mutations.

Droupadi et al. (1992) approximated the change in free energy from van't Hoff plots to be −9.8 kcal/mol. Our calculated changes in electrostatic free energy upon complex formation of the wild-type structure is −1.43 kcal/mol (Fig. 9). We can explain the calculated  $\Delta G_{elec}$  over the entire pH range using the same arguments of previous work in our laboratory studying antibody, lysozyme complexes (Gibas and Subramaniam, 1997). In this study, lysozyme binding was mediated by salt bridge formation between two glutamate residues (also at H:35 and H:50) and two arginine residues of the antigen. At very low pH, Glu H:35 and Glu H:50 are protonated. Complex formation then requires the burial of the positively charged hapten with no counter ions present, thus the  $\Delta G_{elec}$  is large and positive. At very high pH, the ionized group is solvent exposed, and complex formation only requires the burial of the neutral portion of the hapten. There exists a sharp increase in the  $\Delta G_{elec}$  between pH 1.5–3.0 which occurs from forcing the ionized guanidinium to be proximal to the protonated Glu H:35 and Glu H:50.

### 3.7. pH-dependent association energetics of selected mutants

Table 6 summarizes how mutating residues near the active site affect the pH-dependent association energetics. Control mutation data is included to ensure the

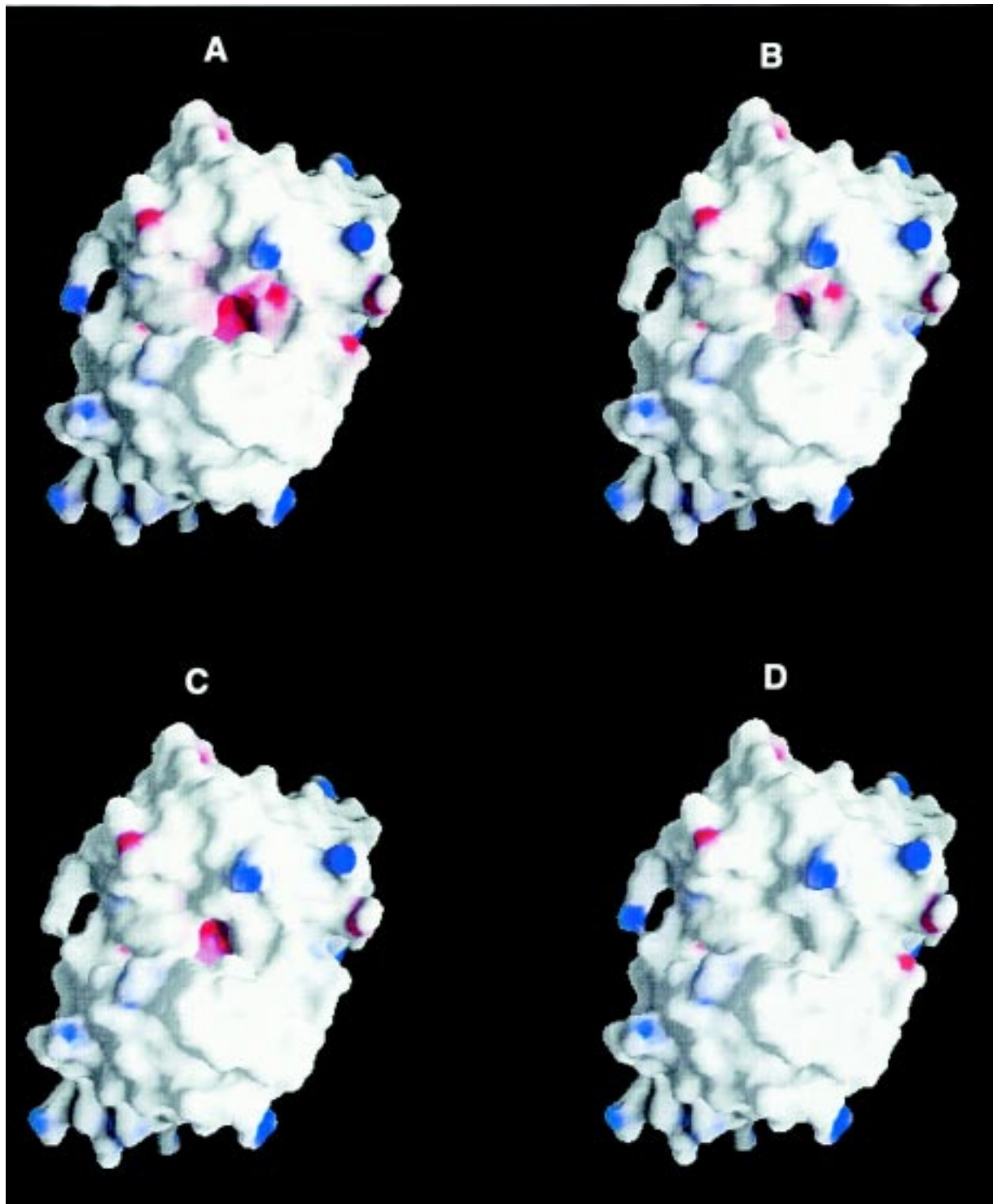


Fig. 8. Electrostatic potential maps generated from the program GRASP showing charge distribution on the surface of four apoprotein structures. (A) Wild-type NC6.8. (B) E(H:35)Q NC6.8. (C) E(H:50)Q NC6.8. (D) E(H:35)Q, E(H:50)Q NC6.8.

reliability of our approach. The double mutation of Glu H:35 and Glu H:50 to glutamine residues has the largest destabilizing effect. The number of mutations that lead to electrostatically stabilizing complex formation is very surprising. Further experimental work

must be carried out to determine if modeling only the electrostatic component of the free energy accurately accounts for the relative stability of the mutants.

The changes in the  $\Delta G_{\text{elec}}$  listed in Table 6 are calculated using the equation

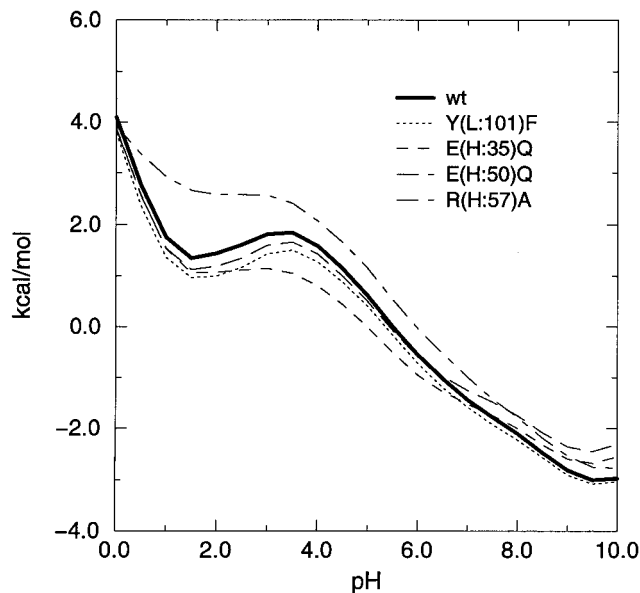


Fig. 9. Change in electrostatic free energy on binding ( $G_{\text{elec,complex}} - (G_{\text{elec,free antibody}} + G_{\text{elec,hapten}})$ ) vs pH for the wild-type, Y(L:101)F, E(H:35)Q, E(H:50)Q, and R(H:57)A structures. (The changes in electrostatic free energy of all mutants calculated are listed in Table 6.)

$$(G_{\text{elec,wt,complex}} - G_{\text{elec,mutant,free Ab}}) - (G_{\text{elec,wt,complex}} - G_{\text{elec,mutant,free Ab}}) \quad (7)$$

Therefore, the changes arise from both the differences in the electrostatic environment due to complex formation and the structural rearrangement that accompanies the association. With the exception of the double E(H:35)Q/E(H:50)Q mutant, all  $\Delta\Delta G_{\text{elec}}$  values are similar to the control values. The unexpectedly large control values can be explained by local changes between the unbound and bound structures. For example, the D(L:17)N control mutation results in a  $\Delta G_{\text{elec}}$  change of  $-0.31$  kcal/mol. This change in electrostatic free energies arises from the loss of dipole–dipole interactions between the two structures. The smallest change is in the Y(L:37)F mutation, in which the position of the parent tyrosine residue is unchanged between the two structures.

## 4. Discussion

### 4.1. Acidic residues

The pKa values of Glu H:35 and Glu H:50 are shifted in opposite directions. Glu H:35 becomes more basic on complex formation, whereas Glu H:50 becomes more acidic. Both residues of the complexed structure are calculated to be 0% solvent accessible by Naccess, and are nearly so for the uncomplexed struc-

ture. HBPLUS predicts a hydrogen bond between OE1 of Glu H:50 and N16 of the guanidinium moiety of the sweetener (Fig. 3), however the separation distance is a bit too much for the typical hydrogen bond, and seems to be more of an electrostatic interaction than a hydrogen bond. The interaction between the hapten and Glu H:50 lowers the pKa of the acid and raises the pKa of the guanidinium moiety of the sweetener. Glu H:50 is involved in several hydrogen bonds with Asn H:59. Two hydrogen bonds exist between backbone atoms of the asparagine and backbone atoms of the glutamate, which make up part of the  $\beta$ -barrel motif on the Fab fragment. In addition, the sidechain amide of Asn H:59 is a hydrogen bond donor to OE2 of the Glu H:50. Glu H:50 is also hydrogen bonded to another proximal glutamate residue (Glu H:35) through an OE2–OE1 interaction (2.7 Å). The acidic properties of Glu H:35 act in the same way as Asn H:59 does, stabilizing ionization of Glu H:50. Glu H:35 is quite acidic due to hydrogen bonding with the sidechain N–H of Trp H:47. Glu H:35 is even more acidic when structural waters are included in the pKa calculation. This is because a water molecule (HOH 234) is bound in a position that donates a proton to OE1 of Glu H:35. The consequences of the hydrogen bond is lessened electron density between OE1 and its acidic proton, making the OE2–OE1 hydrogen bond between Glu H:35 and Glu H:50 more energetically favorable. Glu H:35 is also directly interacting with the ligand as implicated by the interaction matrix (Fig. 7). Glu H:35 forms a strong salt bridge with the basic moiety of the ligand.

Among the residues buried inside the protein interior, Asp H:104 is the only one with a change in pKa value on association. However, Asp H:104 is not directly interacting with the hapten or any of the residues that interact with the hapten. The solvent accessibility of Asp H:104 does not change on complex formation. Therefore, the only explanation seems to be long range electrostatic interactions. The pKa of the sidechain carboxylate of Asp H:104 is very low. The sidechain carboxylate of Asp H:104 is involved in a salt linkage with the guanidinium sidechain of Arg H:88, and is hydrogen bonded to the backbone nitrogen of Tyr H:105. In both cases, the aspartate is acting as a proton acceptor, making protonation less favorable.

### 4.2. Basic residues

Arg H:57 is involved in the most conspicuous interaction with the hapten. The guanidinium ion sidechain is linked to the hapten via a salt bridge with the carboxyl moiety of the sweetener. The pKa of Arg H:57 is lowered on complex formation, which is the expected result of the carboxylate's influence, and is a

full pKa unit more basic than arginine peptide in aqueous environment. Arg H:57 is calculated to be 58.5% solvent accessible for the uncomplexed structure, and 47.6% solvent accessible for the complex, resulting in a 10.9% burial of Arg H:57 on complex formation.

His L:31 is involved in three hydrogen bonds with back bone atoms of various residues, none of which are titrating residues. ND1 of His L:31 is hydrogen bonded to Asn L:33, causing NE2 to be titratable nitrogen of the imidazole ring. His L:31 is close enough to hydrophobically contact Tyr L:37 (3.5 Å), although it is doubtful if this is enough to account for His L:31's change in pKa on complex formation. His L:31 is 31.9% solvent accessible in the uncomplexed structure. Complex formation buries 10.1% of the basic residue with NE2 accounting for the bulk of the residue's accessibility. As the local dielectric lowers on complex formation, the equilibrium shifts towards neutral imidazole.

#### 4.3. Combining site tyrosine residues

Complex formation has significant effects on the pKa values of four combining site tyrosine residues (Table 2). Tyr L:37 is much more acidic than the other tyrosine residues at the combining site. This is due to the fact that Tyr L:37 is a hydrogen bond acceptor for the sidechain amide of a proximal asparagine residue. Complex formation causes the pKa to increase. Tyr L:37 is 8.4% solvent accessible in the uncomplexed structure and 3.7% accessible in the complexed structure. However, complex formation results in a significant loss (11.9%) of solvent accessibility for the phenolic oxygen atom. Thus, the lower dielectric is shifting the acid/base equilibrium away from ionization.  $\pi$ -stacking interactions are not possible explanations because the plane of the two aromatic groups are nearly perpendicular to one another, and are separated by more than 4 Å.

When structural water molecules are included, HBPLUS predicts that Tyr L:41 is hydrogen bonded to the cyano nitrogen of the ligand through a bridging structural water (HOH 242). HOH 242 is 2.8 Å away from the cyano nitrogen which is exactly the optimal distance for an electrostatic bond. Tyre L:41 is completely solvent inaccessible in the complexed structure, and is less than 1% solvent accessible on dissociation.

It has been reported elsewhere (Droupadi and Linthicum, 1995) that Tyr L:101 forms contacts with the *p*-cyanophenyl ring of the ligand on complex formation. The distances between the two rings is less than 4 Å, while the angle between the two aromatic rings is only 11°. That  $\pi$ -stacking interactions are necessary for high potency is shown by experimental results from sweeteners without the *p*-cyanophenyl moiety. Our results support the experimental obser-

vations. The Tyr L:101, guanidinium interaction was calculated to be the most favorable protein, ligand interaction. The *p*-cyanophenyl ring is polar and on association induces electronic rearrangement of the phenolic Tyr L:101. The electronic rearrangement on complex formation should result in an electronic rearrangement with an increased electron density about the electron deficient cyano group. This results in lessened electron density about the phenolic oxygen, making the alcohol more acidic. However, this is competing with the change in the local dielectric on burial of the ligand. Complex formation lowers the solvent accessibility of the titratable oxygen by 13.11 Å<sup>2</sup>, thus lowering the local dielectric.

The backbone carbonyl of Tyr H:100 is predicted by HBPLUS to be a hydrogen bond acceptor from N15 of the hapten. Whether or not this hydrogen bond actually exists is not certain. For the right stereochemistry, the proton would have to come out of the plane of the guanidinium a few degrees such that the proton is orientated in a way that the carbonyl could act as a hydrogen bond acceptor. We note here that guanidinium is not planar, in fact N15 is approaching a tetrahedral geometry. Whether this is an artifact of crystallization or complex formation puckers of the guanidinium group is yet to be determined. Tyr H:100 is 77.2% solvent accessible in the uncomplexed structure. Complex formation buries 31.6% of the residue, of which 5.60 Å<sup>2</sup> are from the phenolic oxygen.

#### 4.4. Other key residues

In addition to the above nine residues implicated by Fig. 5, two non-titrating residues are key to stable complex formation. Asn H:59 has already been implicated in stabilization of the ionization of Glu H:50. Asn H:59 is also in direct contact with the hapten. The amide sidechain of the asparagine is a hydrogen bond donor to the carboxyl moiety of the sweetener. The mutation of Asn H:59 to an aspartic acid would have the same hydrogen bonding characteristics, but would upset the delicate charge balance at the combining site. Ser L:94, like Tyr L:41 is also hydrogen bonded to the cluster of four structural waters. The serine is hydrogen bonded to HOH 242 and HOH 229, both of which are sufficiently close to have dipole–dipole interactions with the polar cyano group.

#### 4.5. Changes in pKa values of selected mutants

Mutation of Glu H:35 and Glu H:50 to glutamine residues disrupts the charge balance of the combining site. The E(H:35)Q mutation causes several residues to be more acidic. With the loss of the anionic residue and its interaction with the basic moiety of the ligand, the interactions between Glu H:50 and the ligand are

even more important, causing H:50 to be more acidic. The pKa value of the ligand's guanidinium group is shifted towards neutral as a result of the loss of the stabilizing Glu H:35, guanidinium interaction. In the wild-type structure, the pairwise electrostatic potential between Glu H:35 and Tyr L:41 and between Glu H:35 and Tyr L:101 is significantly repulsive (Fig. 7). The E(H:35)Q mutation alleviates the repulsive pairwise potentials, causing both tyrosine residues to be more acidic.

Mutation of H:50 to glutamine has similar effects as the E(H:35)Q mutation. The Glu H:50 mutation causes Glu H:35 to be more acidic in order to compensate for the loss of the stabilizing Glu H:50, guanidinium interaction. Mutation of H:50 has a larger destabilizing effect on the guanidinium group than the mutation of H:35. This is expected due to the more stabilizing pairwise potential between H:50 and the guanidinium in the native structure. In the native structure, the pairwise potential between Glu H:50 and Tyr L:101 is also repulsive (whereas the potential between Glu H:50 and Tyr L:91 is neutral), and mutation of the acid to the amide makes ionization of the tyrosine more stable.

Mutating Arg H:57 to an alanine causes the pKa of the carboxyl moiety to be shifted towards neutral. In the wild-type complex, the pKa of the carboxyl moiety is 0.733 pH units. This facilitates salt bridge formation with the side chain of the arginine. The ability to form the salt bridge is destroyed in the R(H:57)A mutant, and the carboxyl pKa value is shifted towards that of the free ligand. The pKa value of Glu H:50 is also affected by the R(H:57)A mutation. The pKa value of Glu H:50 is shifted towards neutral by the mutation. This can be explained by the loss of stabilizing interaction between Glu H:50 and Arg H:57 in the wild-type complex.

Each of the tyrosine residues at the combining site were mutated to phenylalanine residues. Mutation of the key Tyr L:101 has different effects on each of the two key glutamate residues. The pairwise electrostatic potential matrix between Tyr L:101 and each of the glutamates is repulsive. The repulsive interaction in the wild-type structure between H:50 and L:101 is however larger, and hence, the loss of this repulsive potential stabilizes ionization of H:50. Because the pairwise potential between H:35 and the tyrosine is of the same sign as the H:50, L:101 potential, one would expect the pKa of H:35 to be shifted towards ionization as well. However, this is not the case, suggesting more complex interaction relationships. The repulsive potential H:50 and L:101 is almost twice that of the potential between H:35 and L:101. On mutation of L:101 to a nontitrating residue, the repulsive pairwise potential is lost, making ionization of H:50 more favorable. In the wild-type complex, there is also a strong repulsion

between H:50 and H:35 (2.00 kcal/mol). When H:50 becomes more acidic on mutation of the tyrosine, ionization of H:35 is less favorable, shifting the pKa value towards neutral. The effect of the Y(L:101)F mutation is as expected on the pKa of the guanidinium group. By eliminating the very energetically favorable interaction, guanidinium ionization is less favorable, shifting the pKa towards neutral.

#### 4.6. Summary

In conclusion, continuum electrostatics methods provide an efficient and accurate means of calculating individual residue pKa values. These methods can be applied to a variety of antibody, antigen systems in order to better understand the pH dependence of association. In mAb NC6.8 studies, continuum electrostatics calculations reveal that both charge complementarity and aromatic interactions are necessary for specificity. Calculations on several mutant structures suggest potential mutagenesis experiments which will shed further light on the forces that drive association has provided a short list of potential experimental structures that we wish to study. Included in this list is mutating both Glu H:35 and Glu H:50 to the neutral glutamine isochores as well as modifying the stereochemistry by changing them to aspartate residues. Other experiments include mutating of the key aromatic ( $\pi$ -stacking residues) to other aromatic homologs and aliphatic residues.

#### Acknowledgements

The authors would like to thank Dr Cynthia Gibas for her helpful discussions on computational issues of the continuum electrostatics calculations; Dr Andrew McCammon for providing the UHBD suite of programs, for the calculation of the pKa values; and Dr Barry Honig for providing the program GRASP, for the display of electrostatic potentials. This work was supported by National Science Foundation Grant DBI 96-04223 and National Institutes of Health Grant R01 GM 46535.

#### References

- Alegre, M.L., Collins, A.M., Pulito, V.L., Brosius, R.A., Olson, W.C., Zivin, R.A., Knowlew, R., Thistlethwaite, J.R., Jolliffe, L.K., Bluestone, J.A., 1992. Effect of a single amino acid mutation on the activating and immunosuppressive properties of a 'humanized' OKT3 monoclonal antibody. *J. Immunol.* 148, 3461–3468.
- Anchin, J.M., Linthicum, D.S., 1993. Variable region sequence and characterization of monoclonal antibodies to a

- N,N',N''trisubstituted guanidine high potency sweetener. *Molec. Immunol.* 30, 1463–1471.
- Antosiewicz, J., McCammon, J.A., Gilson, M.K., 1994. Prediction of pH-dependent properties of proteins. *J. Mol. Biol.* 238, 415–436.
- Benjamin, D.C., Williams Jr, D.C., Smith-Gill, S.J., Rule, G.S., 1992. Long-range changes in a protein antigen due to antigen-antibody association. *Biochemistry* 31, 9539–9545.
- Boresch, S., Archontis, G., Karplus, M., 1994. Free energy simulations, the meaning of the individual contributions from a component analysis. *Proteins, Struct. Funct. Genet.* 20, 25–33.
- Boresch, S., Karplus, M., 1995. The meaning of component analysis, decomposition of the free energy in terms of specific interactions. *J. Mol. Biol.* 254, 801–807.
- Brady, G.P., Szabo, A., Sharp, K., 1996. On the decomposition of free energies. *J. Mol. Biol.* 263, 123–125.
- Brooks, R.B., Brucoleri, R.E., Olafson, B.D., States, D.J., Swaminathan, S., Karplus, M., 1983. CHARMM, A program for macromolecular energy, minimization, and dynamics calculations. *J. Comput. Chem.* 4, 187–217.
- Chacko, S., Silverton, E.W., Smith-Gill, S., Cohen, G., Davies, D., 1995. Structure of an antibody-lysozyme complex unexpected effect of a conservative mutation. *J. Mol. Biol.* 245, 261–274.
- Chothia, C., Lesk, A.M., 1987. Canonical structures for the hypervariable regions of immunoglobins. *J. Mol. Biol.* 196, 901–917.
- Davies, D.R., Metzger, H.A., 1983. Structural basis of antibody diversity. *Ann. Rev. Immunol.* 1, 87–117.
- Droupadi, P.R., Anchin, J.M., Meyers, E.A., Linthicum, D.S., 1992. Spectrofluorimetric study of the intermolecular complexation of monoclonal antibodies with the high potency sweetener N-(p-cyanophenyl)-N'-(diphenylmethyl)guanidineacetic acid. *J. Mol. Recog.* 5, 173–179.
- Droupadi, P.R., Linthicum, D.S., 1995. Absorption spectroscopy of the complexation between superpotent guanidinium sweeteners and specific monoclonal antibodies. *Int. J. Biochem. Cell Biol.* 27, 351–357.
- Gibas, C.J., Subramaniam, S., 1996. Representation of local environments in protein pKa calculations. *Biophys. J.* 71, 138–147.
- Gibas, C.J., Subramaniam, S., 1997. pH dependence of antibody/lysozyme complexation. *Biochemistry* 36, 15,599–15,614.
- Gilson, M.K., 1993. Multiple-site titration and molecular modeling, two rapid methods for computing energies and forces for ionizable groups in proteins. *Proteins, Struct. Funct. Genet.* 15, 266–282.
- Guddat, L., Shan, L., Anchin, J., Linthicum, D.S., Edmundson, A.B., 1994. Local and transmitted conformational changes on complexation of an anti-sweetener Fab. *J. Mol. Biol.* 236, 247–274.
- Hubbard, S.J., Campbell, S.F., Thornton, J.M., 1991. Conformational analysis of limited proteolytic sites and serine proteinase protein inhibitors. *J. Mol. Biol.* 220, 507–530.
- Jorgensen, W.L., Tirado-Rives, J., 1988. The OPLS potential function for proteins, energy minimizations for crystals of cyclic peptides and crambin. *J. Amer. Chem. Soc.* 110, 1657–1666.
- Kozack, R.E., d'Mello, M.J., Subramaniam, S., 1995. Computer modeling of Electrostatic Steering and Orientational Effects in antibody-antigen association. *Biophys. J.* 68, 807–814.
- Knossow, M., Daniels, R.S., Douglas, A.R., Skehel, J.J., Wiley, D.E., 1984. Three-dimensional structure of an antigenic mutant of the influenza hemoglobin. *Nature* 311, 678–680.
1992. In: Dean, J. (Ed.), *Langes Handbook of Chemistry*, 14th ed. McGraw-Hill, New York, p. 8.47.
- Madura, J.D., Briggs, J.M., Wade, R.C., Davis, M.E., Luty, B.A., Ilin, A., Antosiewicz, J., Gilson, M.K., Gagheri, B., Scott, L.R., McCammon, J.A., 1995. Electrostatics and diffusion of molecules in solution, simulations with the University of Houston Brownian Dynamics program. *Comput. Phys. Commun.* 91, 57–95.
- McDonald, I.K., Thornton, J.M., 1994. Satisfying hydrogen bonding potential in proteins. *J. Mol. Biol.* 238, 777–793.
- Morokuma, K., 1977. Why do molecules interact? The origin of electron donor-acceptor complexes, hydrogen bonding and proton affinity. *Acc. Chem. Res.* 10, 294–300.
- Muller, G.W., Walters, D.E., DuBois, G.E., 1992. N,N'-Disubstituted guanidine high-potency sweeteners. *J. Med. Chem.* 35, 740–743.
- Padlan, E.A., 1990. On the nature of antibody combining sites, unusual structural features that may confer on these sites an enhanced capacity for binding ligands. *Proteins, Struct. Funct. Genet.* 7, 112–124.
- Padlan, E.A., 1994. Anatomy of the antibody molecule. *Molec. Immunol.* 31, 169–217.
- Poljak, R.J., Amzel, L.M., Chen, B.L., Phizackerley, R.P., Saul, F., 1973. Three dimensional structure of the Fab fragment of a human immunoglobulin at 2.8 Å resolution. *Proc. Nat. Acad. Sci. USA* 70, 3305–3310.
- Shrake, A., Rupley, J.A., 1957. Environment and exposure to solvent of protein atoms. Lysozyme and insulin. *J. Mol. Biol.* 79, 351–371.
- Schellman, J.A., 1975. Macromolecular binding. *Biopolymers* 14, 999–1018.
- Tanford, C., Roxby, R., 1972. Interpretation of protein titration curves, application to lysozyme. *Biochemistry* 11, 2192.
- Tello, D., Goldblum, F.A., Mariuzza, R.A., Ysern, X., Schwarz, F.P., Poljak, R.J., 1993. Three-dimensional structure and thermodynamics of antigen binding by antilysozyme antibodies. *Biochem. Soc. Trans.* 21, 943–946.
- Tetin, S.Y., Linthicum, D.S., 1996. Circular dichroism spectroscopy of monoclonal antibodies that bind a superpotent guanidinium sweetener ligand. *Biochemistry* 35, 1258–1264.